frontiers | Frontiers in Earth Science

TYPE Original Research
PUBLISHED 31 July 2024
DOI 10.3389/feart.2024.1445918

Check for updates

OPEN ACCESS

EDITED BY
Fan Yang,
Lanzhou University, China

REVIEWED BY
Chang-Hao Xiao,
Institute of Geomechanics Chinese Academy of Geological Sciences, China
Liang Qiu,
China University of Geosciences, China

*CORRESPONDENCE
Shahram Shafieibafti,
shafiei_shahram@uk.ac.ir
Reza Derakhshani,
r.derakhshani@uu.nl

RECEIVED 08 June 2024
ACCEPTED 01 July 2024
PUBLISHED 31 July 2024

CITATION
Dorzadeh H, Shafieibafti S, Keshavarz S, Omrani J, Rashidi A, Nemati M and Derakhshani R (2024), Calcite e-twins as a tectonic indicator, paleo stress pattern and structural evolution of the Zagros hinterland, SE Iran.
Front. Earth Sci. 12:1445918.
doi: 10.3389/feart.2024.1445918

Calcite e-twins as a tectonic indicator, paleo stress pattern and structural evolution of the Zagros hinterland, SE Iran

Hamed Dorzadeh[1], Shahram Shafieibafti[1]*, Saeede Keshavarz[2], Jafar Omrani[3], Ahmad Rashidi[4], Majid Nemati[1,4] and Reza Derakhshani[1,5]*

[1]Department of Geology, Faculty of Sciences, Shahid Bahonar University of Kerman, Kerman, Iran, [2]Department of Earth Sciences, Graduate University of Advanced Technology, Kerman, Iran, [3]Geological Survey and Mineral Exploration of Iran, Tehran, Iran, [4]Department of Earthquake Research, Shahid Bahonar University of Kerman, Kerman, Iran, [5]Department of Earth Sciences, Utrecht University, Utrecht, Netherlands

Through the examination of calcite twins, this research outlines the tectonic development and paleo stress patterns of the Paleozoic Routshon complex situated in the southeastern segment of the Sanandaj–Sirjan zone, a hinterland region of the Zagros orogeny in southeastern Iran. The study of orogenic phase indicates that the deformation event affecting the southern sector of the Sanandaj-Sirjan zone aligns with the Cimmerian orogenic phase of the Late Triassic period. A variety of structural features at both map and outcrop scales highlight the importance of slip partitioning in the structural evolution of this region, driven by inclined transpression. Observations suggest that the deformation related to contractional components includes steeply to moderately plunging folds, dip-slip domain deformation primarily involving thrusts, and ongoing deformation by strike-slip component motion, which results in thrust-related ductile shear zones. The analysis of calcite c-axis fabrics from mylonite samples obtained from these shear zones indicates a low-temperature monoclinic pattern of non-coaxial deformation. This deformation type underscores the impact of the strike-slip component in the development of progressive simple shear within thrust-related shear zones in this segment of the Sanandaj-Sirjan zone. Dynamic analysis of c-axis fabric data reveals a NE-SW orientation for the principal compressive axes (σ1) in this area. This direction, corroborated by additional data such as fault surface, GPS, and earthquake focal mechanism data, confirms that the orientation of the compressive axes (σ1) has remained consistent from the Late Triassic to the present.

KEYWORDS

calcite twinning, mylonite fabric, Sanandaj-Sirjan zone, structural geology, tectonics

1 Introduction

Mechanical e-twinning of calcite represents the primary mechanism of crystal-plastic deformation in coarse-grained limestones and marbles subjected to temperatures below approximately 400°C (Turner, 1953). Twins have been extensively utilized as markers of deformation history, providing valuable insights into the stress regimes that shaped geological formations (Turner and Weiss, 1963), who developed a dynamic technique to

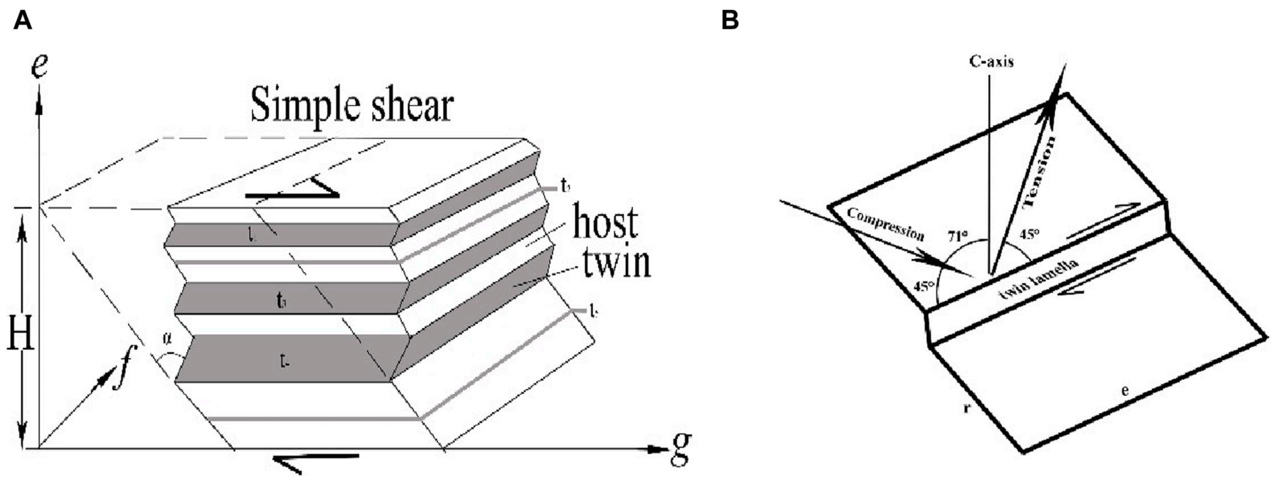

FIGURE 1
(A) Schematic of twin structures in a calcite grain caused by simple shear (Evans and Groshong, 1994) showing the f-axis aligned perpendicular to the ge plane. Dashed lines represent the boundary of the original untwinned calcite grain, with shaded regions indicating the twinned lamellae and unshaded regions showing the host calcite. The angle of rotation (α) from the host portion to the twinned lamellae is measured at 38°17 (Handin and Griggs, 1951) H represents the total thickness of the host and twins combined, and t specifies the thickness of the twin (Jamison and Spang, 1976). **(B)** Diagram illustrating the geometry of an e-twin in calcite, highlighting the orientations of compression and tension axes (Shelley, 1993).

deduce stress axes from a population of e-lamellae in deformed calcite rocks (Figure 1). This technique has been subsequently modified and refined to ascertain the principal direction and/or magnitudes of paleo-stress and numerous studies have refined techniques to deduce principal stress directions and magnitudes from calcite twin data (Lacombe and Laurent, 1992; 1996; Burkhard, 1993; Parsons and Thompson, 1993; Shelley, 1993; Lacombe, 2001; 2007; Jaya and Nishikawa, 2013; Yamaji, 2015; Qiu et al., 2016; 2022; Shan et al., 2019; Zheng and Shan, 2020).

The scientific issue in the study area revolves around the complex tectonic evolution and paleo stress patterns within the Routshon complex, part of the Sanandaj–Sirjan zone in southeastern Iran. This region, a hinterland of the Zagros orogeny, exhibits a multifaceted geological history influenced by the prolonged convergence between Eurasia and Gondwanaland fragments, as evidenced by ophiolite belts and current GPS vectors (Agard et al., 2011). Despite its significance, the tectonic processes and stress regimes that have shaped this area remain poorly understood, particularly regarding the role of slip partitioning and inclined transpression in its structural evolution.

To address these issues, our research focuses on a detailed analysis of calcite twinning and c-axis fabrics from mylonite samples within thrust-related shear zones in the Routshon complex. Previous studies have identified key structural features and deformation phases in the Zagros region (Berberian and King, 1981; Alavi, 2004), but comprehensive paleo stress analyses integrating these findings with modern techniques are lacking.

In this study, we performed a dynamic analysis of c-axis fabric data to map out the principal compressive axes (σ1) and their orientations. By examining calcite twins and their deformation patterns, we aimed to reconstruct the paleo stress fields and elucidate the tectonic history of the region. Our approach combines field observations, microstructural analysis, and stereographic projections to provide a nuanced understanding of the stress regimes that have influenced the geological evolution of the Routshon complex.

Our findings indicate that the deformation events in the southern Sanandaj–Sirjan zone align with the Cimmerian orogenic phase of the Late Triassic period, characterized by contractional components and strike-slip motions resulting in ductile shear zones. The NE-SW orientation of the principal compressive axes (σ1), corroborated by fault surface GPS and earthquake focal mechanism data, highlights the consistency of the stress regime from the Late Triassic to the present.

This paper aims to utilize the properties of calcite twins to investigate the paleo-stress patterns and structural evolution of the Paleozoic Routshon complex, which is exposed in the Bazar area (Figure 2) within the Sanandaj-Sirjan Zone (SSZ), southeastern Iran. The study seeks to provide insights into the tectonic evolution of the Zagros orogenic belt's hinterland.

2 Geological setting

The Zagros orogeny is part of the Alpine–Himalayan belt system, formed due to the prolonged convergence between Eurasia and fragments derived from Gondwanaland, as evidenced by ophiolite belts and current GPS vectors (Agard et al., 2011). This orogenic belt comprises southwest-verging mountains, which developed from the persistent subduction of the Neo-Tethyan oceanic lithosphere from the Jurassic to the Cenozoic era, followed by the collision of the Arabian plate with the Central Iranian microplate in the Cenozoic (Berberian and King, 1981; Alavi, 2004; Kamali et al., 2023). This process is the primary cause of the region's activity, as evidenced by seismic events and morphotectonic features (Derakhshani and Eslami, 2011; Kermani et al., 2017; Rahbar et al., 2017). The formation of this orogeny is attributed to the closure of the Neotethys, following the complete subduction of oceanic crust at a northeast-dipping subduction zone beneath

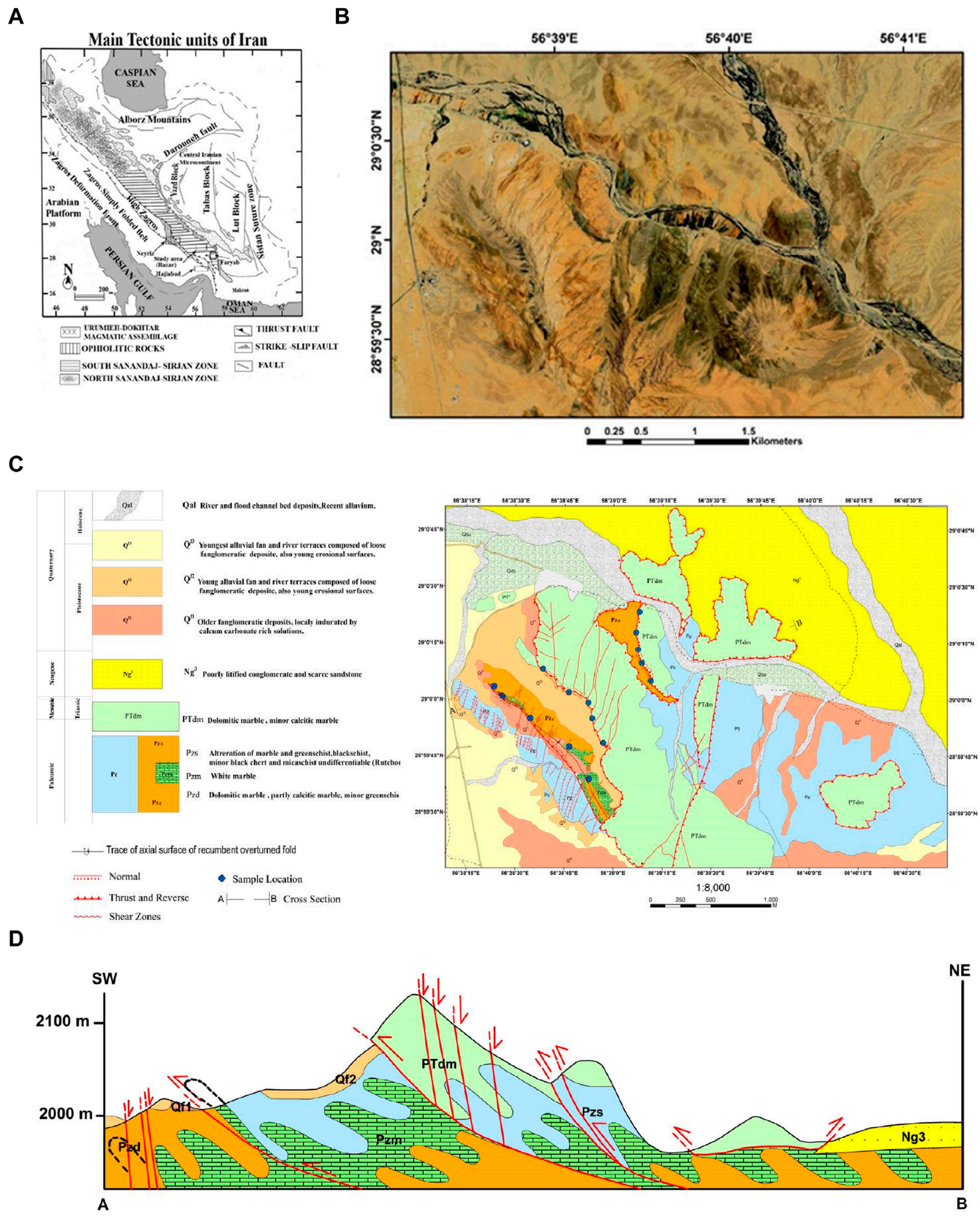

FIGURE 2
(A) Simplified tectonic map of Iran, showing the Sanandaj-Sirjan Zone (SSZ) between the Urumieh-Dokhtar Magmatic Assemblage (UDMA) and the Zagros Fold-Thrust Belt. **(B)** Satellite image of the Bazar area, highlighting major geological features. **(C)** Key structures within the region in map view and **(D)** in cross section view, providing a detailed view of fault lines and thrust systems critical to the area's tectonic framework.

central Iran, and the subsequent Cretaceous continental collision between the Afro-Arabian and Iranian continental fragments (Shafieibafti et al., 2011). The orogenic structure includes: (1) the Mesopotamian–Persian Gulf foreland basin, (2) the Zagros Fold–Thrust belt extending from southwest to northeast (Falcon, 1961; Ghanbarian and Derakhshani, 2022b), (3) the SSZ (Stocklin, 1968), and (4) the Urumieh–Dokhtar Magmatic Assemblage, (UDMA). In contrast to the more extensively studied active tectonics

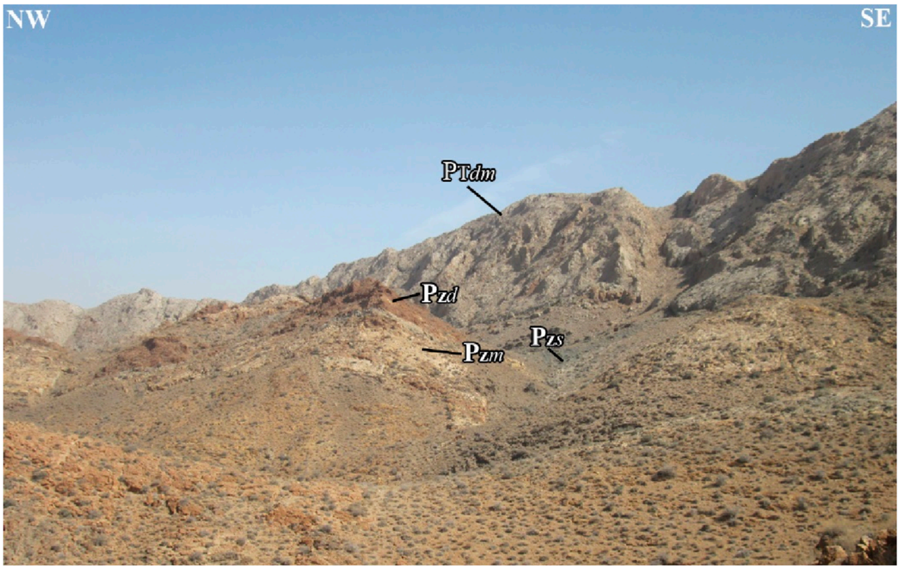

FIGURE 3
Outcrop view of rock units in the study area. Paleozoic units are identified as Dolomites (P_zd), Schists (P_zs), and White Marbles (P_zm). The transitional paleozoic-Triassic unit (P_Tdm) is characterized by Dolomitic marbles, illustrating the lithological diversity and stratigraphic relationships crucial to understanding the region's geological history.

and foreland deformation, there is less knowledge about the hinterland subduction-related arcs parallel to the Zagros, specifically SSZ and UDMA (Agard et al., 2011; Ghanbarian and Derakhshani, 2022a) (Figure 2A). The SSZ and UDMA, located northeast of the Main Zagros Thrust, are believed to result from a northeast-dipping subduction process of the Neo-Tethyan oceanic crust beneath the Iranian continental active margin (Berberian and King, 1981; Amirihanza et al., 2018).

The SSZ stretches approximately 1,500 km from the northwest (Sanandaj) to the southeast (Sirjan) with a width of 150–200 km, running parallel to the Zagros Fold Thrust belt. This zone contains the most intensely deformed rocks, exhibiting a NW-SE structural trend. The southern boundary of the SSZ is defined by the Zagros Main Thrust, which separates it from the Zagros region. Additionally, Central Iran is divided from the SSZ by a series of steep and straight faults, including the Tabriz and Nain-Baft Faults (Şengör and Kidd, 1979; MohammadiNia et al., 2024). The SSZ is characterized by a scarcity of Tertiary volcanic rocks, significant volumes of Mesozoic (and some Tertiary) intrusions, a relatively high abundance of Paleozoic volcanic rocks (Silurian, Devonian, and Permian), and metamorphism due to Cimmerian movements (Aghanabati, 2004; Ghasemi and Talbot, 2006). These features distinguish the SSZ from other geological and structural subdivisions in Iran (Ghazi and Moazzen, 2015). The geodynamic evolution of this zone was driven by the opening and subsequent closure of the Neotethys Ocean along the northeastern margin of Gondwana (Alavi, 1994).

The Sanandaj–Sirjan zone's polyphase deformation structures align with transpressional forces due to the angled collision between the African–Arabian continent and the Iranian microcontinent (Mohajjel and Fergusson, 2000; Sarkarinejad and Azizi, 2008; Sarkarinejad et al., 2008; Shafieibafti and Mohajjel, 2015; Ghanbarian et al., 2021; Mansouri et al., 2021). This transcurrent component arises from an oblique factor in the subduction zone (Shafieibafti, 2007; Sheikholeslami et al., 2008; Shafieibafti and Mohajjel, 2015). This study aims to determine the structural characteristics of the Zagros orogen's backcountry by using calcite twinning analyses to map out the ancient stress fields and the depth of deformation within the Routshon complex, located in the southeastern part of the SSZ.

In the southern part of the Sanandaj-Sirjan Zone (SSZ), Paleozoic strata are divided into six syntectonic regional metamorphic complexes, each with varying metamorphic grades and ages. These complexes are overlain by non-metamorphosed Early Jurassic basal conglomerates, which contain metamorphic clasts, as well as volcanic-detrital rocks. The continuity of these complexes has been traced from Hajiabad in the southeast to Neyriz in the northwest (Berberian, 1976). Each complex is further divided into three metamorphic units, listed from top to bottom: (1) the upper complex (low grade), (2) the middle complex (low to medium grade), and (3) the lower complex (high grade). A single sample of Kyanite-Sillimanite schist from the Neyriz area has been dated using the conventional K/Ar radiometric method, yielding an age of 404 ± 8 Ma, corresponding to the Silurian-Devonian boundary (Watters and Sabzehei, 1970). The middle complex contains poorly preserved fragments of crinoid stems, several corals, and a single Bryozoan, with Devonian pollen and spores reported from carbonaceous black schist (Berberian, 1976). The stratigraphic units in the study area, which extends from longitude 56°36′15″E to 56°40′30″E and latitude 28°59′15″N to 29°0′45″N (Figures 2B, C), consist of the Paleozoic-Mesozoic Routshon complex (GSI, 1997b; 1997a; 2007).

Some researchers have suggested that these metamorphic complexes represent Precambrian basement rocks (Stocklin, 1968), while others attribute their syntectonic regional

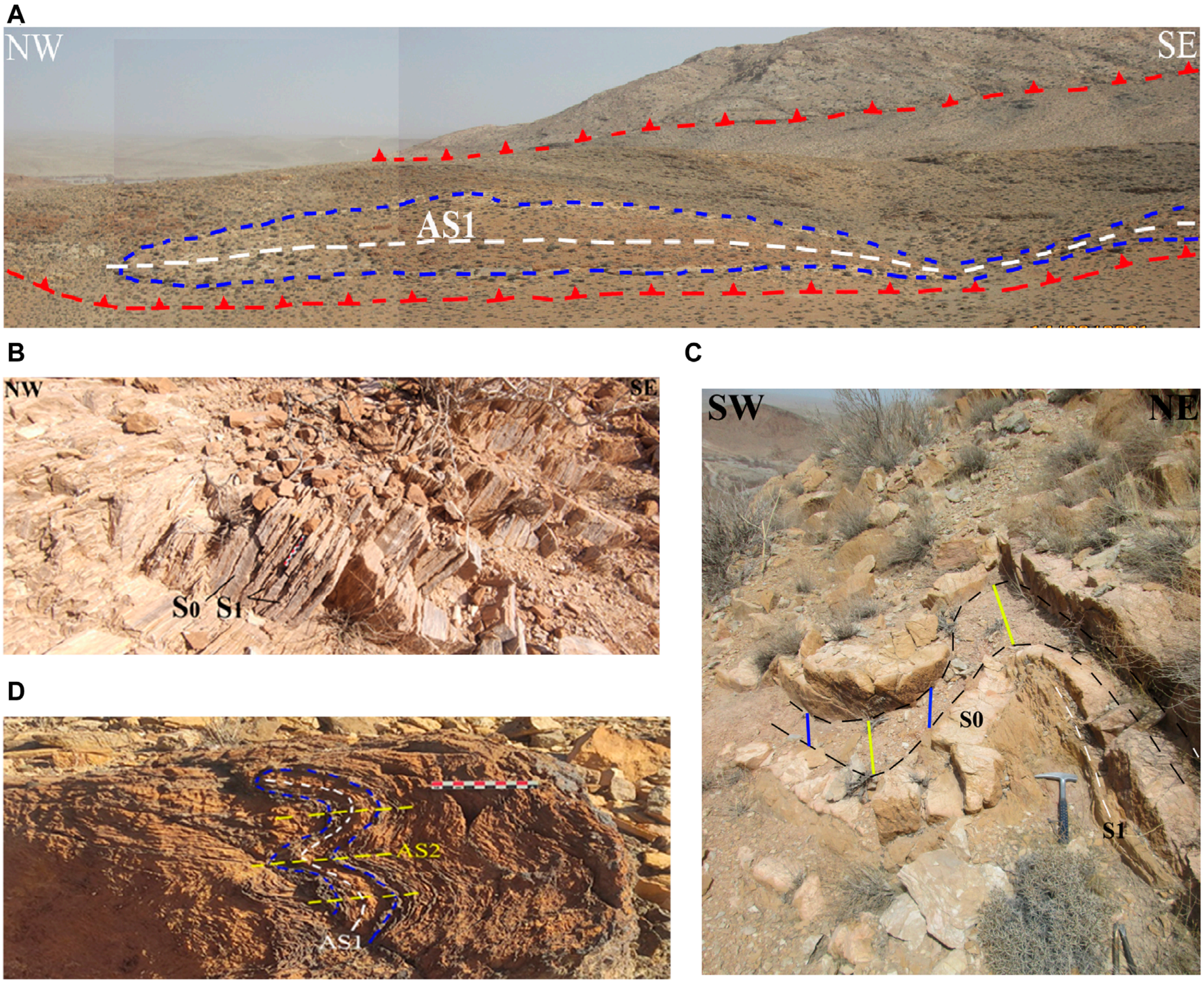

FIGURE 4
(A,B) View of an outcrop featuring an isoclinal fold, highlighting the characteristic features of the F1 folds in the calcite and dolomite marbles (PTd) and white marble (Pm) units of the Routshon complex. The F1 folds are marked by their gently inclined to recumbent geometry with axial planes dipping at angles of 10°–30° toward the NE and axes plunging gently to the W. These folds are indicative of flexural flow deformation. The symbols so and s1 correspond to bedding and schistosity, respectively. **(C)** Under the flexural flow folding mechanism some layers are thickened into axial zones (yellow lines) and thinned into limbs (blue lines) **(D)** Type III interference pattern in folding identified as a Hook type pattern, resulting from the coaxial refolding of F1 and F2 folds.

metamorphism to Early Cimmerian tectonics (Berberian, 1972; 1973; Hushmandzadeh et al., 1972; Majidi, 1972; 1974; Sabzehei and Berberian, 1972; Berberian and Nogol, 1974; Sabzehei, 1974). The Routshon complex includes a variety of rock types such as dolomitic and marble formations, green schists, black schists, chert, mica schists, calcite and dolomite marbles, and white marble (Figure 3).

The Bazar area in the southeastern SSZ exhibits evidence of three distinct deformation events (D1, D2, and D3). Calcite twinning plays a significant role in understanding the deformation mechanisms and stress regimes associated with each phase.

2.1 D1 deformation

The D_1 deformation phase is characterized by folding, manifested in a range from gently inclined to recumbent and spans mesoscopic to macroscopic scales, including axial planar schistosity (Figure 4A). These formations are prominently observed in the calcite and dolomite marbles (PT^d) and white marble (P_m) units of the Routshon complex, as evidenced by detailed field observations and microstructural analysis. Specifically, axial planar schistosity is consistently observed to run parallel to the bedding planes in these units. This parallel alignment is indicative of intense compressive deformation, which is further supported by the presence of well-developed axial planar schistosity, confirmed through microscopic examination of thin sections from multiple samples. These samples exhibit clear evidence of recrystallization and deformation textures consistent with low-grade metamorphic conditions, corroborating the interpretation of the observed fabrics. Our analysis of the F1 folds in the Routshon complex reveals that their axial planes dip at angles of 10°–30° toward the NE, while the fold axes plunge gently to the W. These observations are consistent across multiple outcrops

10.3389/feart.2024.1445918

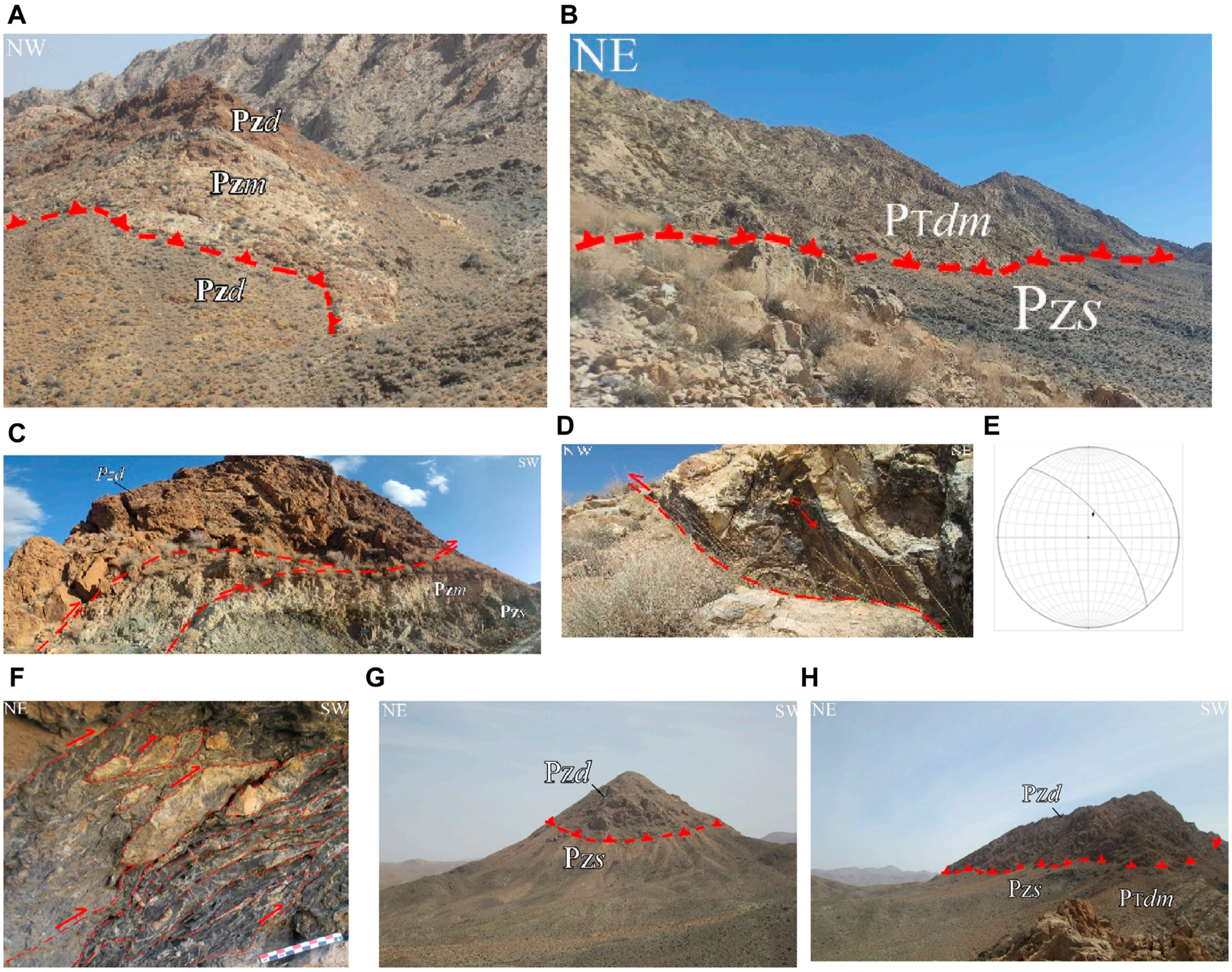

FIGURE 5
(A) Outcrop view of the T_1 thrust, illustrating the truncation and duplication of Dolomites (P_zd). **(B)** Outcrop view of T_2 thrust, where Dolomitic Marbles (Pt*dm*) were truncated and thrusted over schists (P_zs). **(C)** Dolomites (P_zd) overlying the white Marbles (Pz*m*) and Schists (P_zs) by T_3 thrust. **(F)** Flexural-slip duplex structures in the Pzm (white Marbles) and Pzs (Schists) units associated with the T3 thrust, characterized by a sigmoidal configuration and suggesting a southwest thrust direction. **(D,E)** slickenside and striation of T_2 thrust with its stereographic projection (equal area), indicating the direction of movement. **(G,H)** Typical outcrop of klippes, showing Dolomites (P_zd) over Schists (P_zs) by T_4 thrust.

and are supported by detailed field measurements and structural mapping. The gentle plunge of the fold axes and the moderate dip of the axial planes suggest that these folds formed through a process of flexural flow, (Twiss and Moores, 1992; Hatcher, 1995), reflecting the compressive stress regime prevalent during the deformation. In flexural-flow folds, rock material in incompetent layers flows from fold limbs toward fold hinges, and therefore appreciable thickness changes occur in the rock layer. Flexural-flow folds are mostly similar-like folds, but may also include some parallel folds. Some layers in single flexural-flow folds maintain constant thickness; others are thickened into axial zones and thinned into limbs as folding proceeds, indicating a higher contrast in internal ductility. In this area flexural flow evidences are visible in schist in an interbedded marble (Figures 4B, C). At the mesoscopic level, an interference pattern is evident due to the coaxial refolding of F1 folds. While Type I and Type II interference patterns are typically more common, our detailed structural analysis indicates that the overlapping of F1 and F2 folds in the Routshon complex predominantly results in Type III interference patterns. This observation, as outlined by Ramsay and Huber (Ramsay and Huber, 1987), is somewhat unexpected but is supported by consistent field evidence and structural mapping (Figure 4D). The presence of Type III patterns suggests complex deformational histories involving multiple phases of folding and refolding, which we have documented through extensive mesoscopic and microscopic analyses of the fold structures.

2.2 D2 deformation

This deformation event led to the formation of thrust faults (Figure 2). In the hinterlands of orogenic belts, thrusts typically result from differential flow within a ductile mass, which creates F1-folds. Subsequent shearing between the antiform and synform limbs

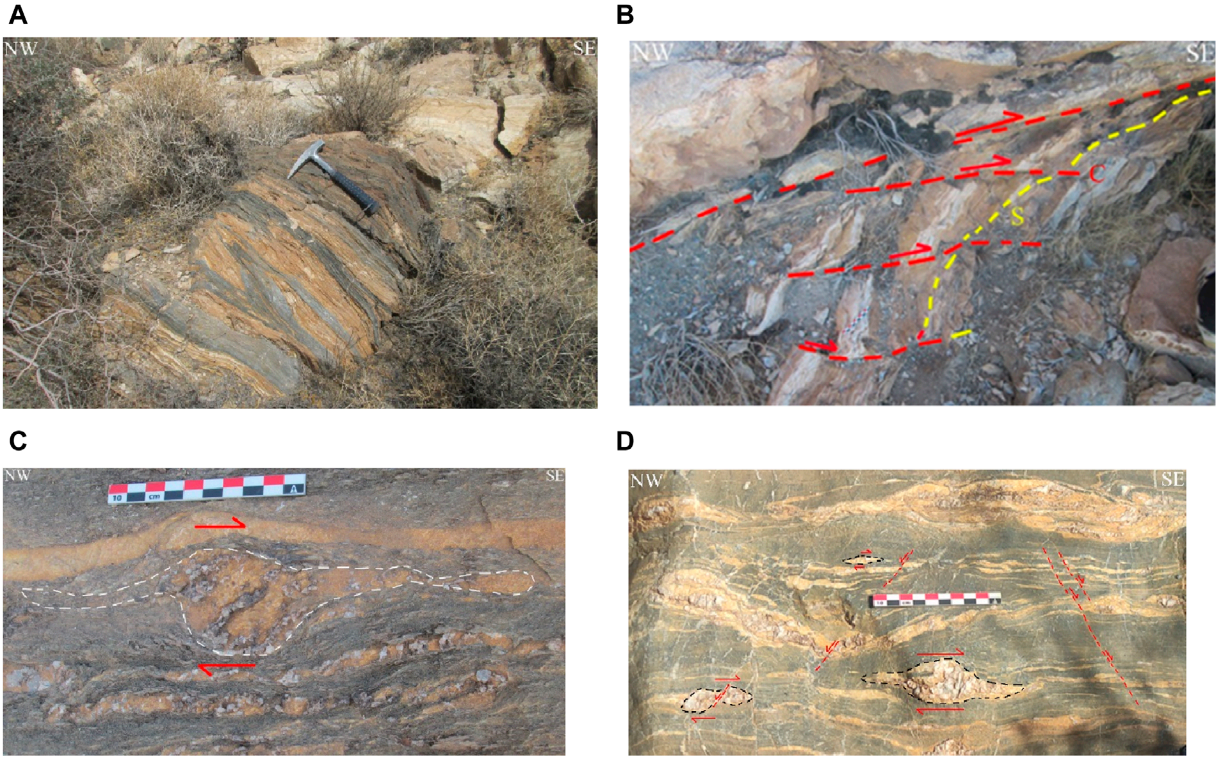

FIGURE 6
(A) Outcrop view of mylonitic foliation within the T_1 thrust shear zone. **(B)** C-type shear band featuring horizontal C-planes and S-planes trending from upper right to lower left. **(C)** δ (delta)- type mantled porphyroclasts. **(D)** σ(Sigma)-type of asymmetric mantled porphyroclats with backward rotation (Zhang and Fossen, 2020) in dolomite and calcite. Also, fractured porohyroclats with and antithetic microfaults evident in these shear zones.

produces these thrusts (Hatcher and Hooper, 1992). In the study area, five thrust sheets (T1–T4), known as the Bazar thrust system, have been identified. These thrust faults influence the complex outcrop patterns and generally trend NW–SE (T1-T4, dipping northeast) or N–S (dipping east) (Figure 2C). Various geological features arise from these faults. The T1 thrust developed along the southern limbs of gently inclined to recumbent F1-folds (Figures 4A, 5A). The overlying of dolomitic marbles (PTdm) atop green schist, black schist, and mica schist (PZs) indicates the influence of the T2 thrust (Figures 5B–D). The T3 thrust involves the thrusting of dolomites (Pzd) over Schists (Pzs) and White Marbles (Pzm), with associated duplex structures in the shear zones (Figures 5E, F). T4 follows an NNE-SSW trend with an easterly dip. The interposition and increasing thickness of the PTdm unit above the Pzd unit due to T4 thrusting and associated shear zones are evident. In the northern region of the T4 thrust, characteristic klippe outcrops are visible (Figures 5G, H).

Shear zones, formed in the thrust sheets, are composed of calcite mylonites. The foliation patterns exhibit east-west orientations and dip northward. The elongation lineation within the calcite mylonites is delineated by the elongated axes of the calcite grains, which are ellipsoidal in shape. The mylonites present multiple shear sense indicators across various scales, all suggesting a right-lateral shear direction, as illustrated in Figures 6A–D.

2.3 D3 deformation

The last deformation phase was characterized by an extensional regime, leading to the formation of normal faults. The bookshelf or domino structures associated with a normal fault can be clearly seen in competence units such as dolomites and marbles (Figure 7). The normal faults show a NNE trend which has a high correlation with dyke orientations. The study area reveals the presence of diacritic dykes within the fault planes, as depicted in Figure 6. The emergence of normal faults is hypothesized to be associated with magmatic activity, a theory that requires more in-depth analysis for verification.

Calcite twinning plays a crucial role in deciphering the deformation history of the Routshon complex across the D1 to D3 phases. During the D1 deformation phase, calcite twins indicate low-temperature compressive conditions, with consistent NE-SW oriented stress axes corresponding to the flexural flow folds. In the D2 phase, the twinning patterns within the mylonitic shear zones of the thrust faults reveal progressive simple shear deformation, providing kinematic indicators of dextral shear. Finally, in the D3 extensional phase, the reorientation of calcite twins reflects the transition to an extensional stress regime, marking the shift from compressional to extensional tectonics. These twinning patterns serve as microstructural markers, offering valuable insights into the

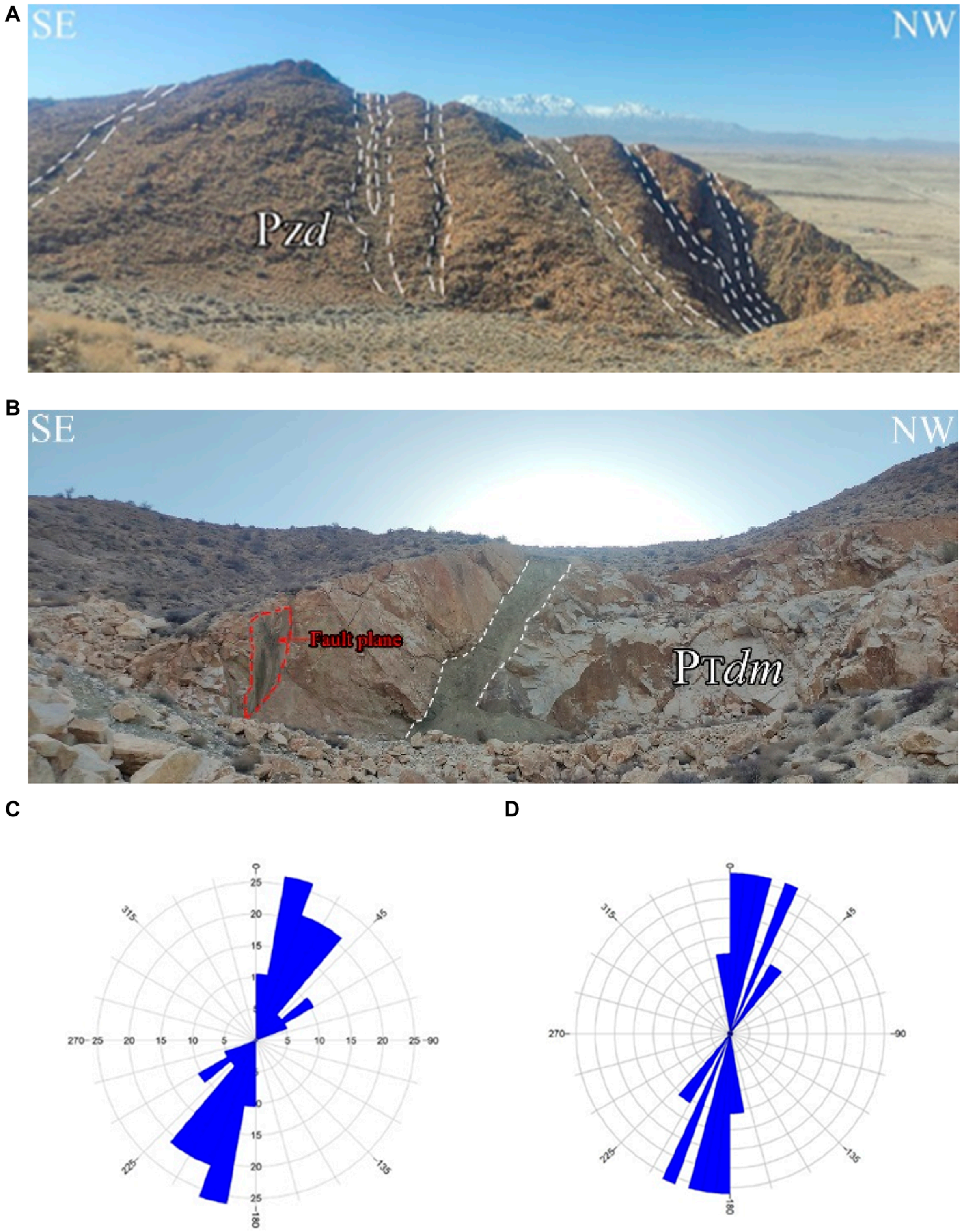

FIGURE 7
(A) Intrusion of dioritic dykes into Dolomites (Pz*d* unit), showing the interaction between magmatic activity and existing rock formations. **(B)** Intrusion of a dioritic dyke into Dolomitic Marbles (P_T*dm* unit) demonstrating the penetration of magmatic material into carbonate units. **(C,D)** Rose diagrams illustrating a high correlation between the trends of normal faults and the orientation of dykes, highlighting the structural relationship between faulting and magmatism.

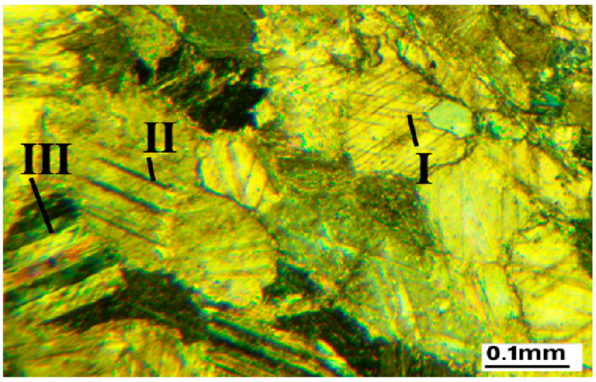

FIGURE 8
Microphotograph (plane-polarized light, PPL) of type I, II and III twins. Type II twins are the predominant twin type observed in mylonitic calcites from the Bazar area.

paleostress orientations and the dynamic tectonic evolution of the study area.

3 Sampling strategy and measurement

To delineate the stress and kinematic chronology of the Sanandaj–Sirjan zone, a sampling strategy was employed that involved collecting 15 oriented samples of calcite mylonites from thrust-related shear zones. These samples were aligned normal to the mylonitic foliation and parallel to its strike. Utilizing a U-stage, measurements were conducted to determine the c-axis and orientation of twin lamellae. Approximately 50 grains were examined per sample. The predominant form of calcite twin lamellae observed was type II twins; however, other twin types were also identified in these samples (as shown in Figure 8). The analysis indicated that 70% of the calcite grains exhibited two sets of twins, while the remaining 30% presented a single set of twins.

4 Discussion

4.1 Structural model of the bazar area

In the southern region of the SSZ, the Paleozoic rock formations underwent deformation and metamorphism as a result of the early Cimmerian orogenic events that occurred in the Late Triassic period. An unconformity between the deformed and metamorphosed Paleozoic complex and the Jurassic units (conglomerate and sandstones) in the Khabr area (east of the study area) and Faryab area (southeast of the study area) reveals the end of the Cimmerian phase (Shafieibafti et al., 2011; Shafieibafti and Mohajjel, 2015). The early Cimmerian deformation along the southern margin of Iran indicates that this region functioned as an active margin during that period (Berberian and King, 1981; Mohajjel et al., 2003; Sheikholeslami et al., 2008). Structures indicative of the early Cimmerian orogenic phase, such as south-southwest verging folds and type C thrusting, are evident (Hatcher and Hooper, 1992), along with thrust-related shear zones under low-grade green-schist metamorphic conditions (Shafieibafti et al., 2011). In various locations within the Sanandaj-Sirjan zone, structural developments consistent with the inclined transpression model have been confirmed (Shafieibafti et al., 2011; Shafieibafti and Mohajjel, 2015; Mansouri et al., 2021). Inclined transpression results from concurrent contraction and oblique-slip shear, which can be decomposed into strike-slip and dip-slip components (Jones, 2004). This model shows that structural evolution, whether through ductile or brittle mechanisms, is closely linked to slip partitioning. The subsequent section will analyze and interpret the structures of the study area using the strain triangle model (Figure 9).

4.1.1 Contractional domain

Deformation related to the contractional component is observed in the calcite and dolomite marbles (PTdm) and white marble (Pzm) units, characterized by folds that range from steeply plunging to moderately inclined (Figures 4A, 9).

4.1.2 Dip-slip domain

In the dip-slip domain, deformation is primarily governed by thrusts dipping north with top-to-the-south movement and thrusts dipping east with top-to-the-west movement. These thrust faults are central to the complexity of the outcrop patterns, typically trending NW–SE or N–S with dips ranging from northeast to east (Figures 2D, 5).

4.1.3 Strike-slip domain

The ongoing deformation under strike-slip component motion is evident in the form of thrust-related ductile shear zones. These zones contain calcite mylonites and display multiple indicators of dextral shear sense (Figures 2D, 5E–H, 9).

4.2 Kinematic interpretation of calcite fabrics

Wenk et al. (1987) classified calcite c-axes fabrics into low-temperature (LT) and high-temperature (HT) categories (Figure 10). LT fabrics, demonstrated in experimental settings, predominantly feature twinning with minor intracrystalline slip as the primary deformation mechanism, whereas HT fabrics are dominated by intracrystalline slip, as seen in experiments. LT fabrics display a distinct peak orientation nearly parallel to the principal stress axes and oblique to the shear plane. This orientation can serve as an indicator of shear sense or as a measure of the degree of non-coaxial deformation. LT fabrics are further differentiated into LT pure shear, where the peak orientation is perpendicular to the shear plane, and LT simple shear, which is similar to LT pure shear but rotated counter to the shear direction. In LT fabrics, the c-axes orientations range from sub-horizontal to gently plunging (Lafrance et al., 1994), presenting a girdle that includes one or two asymmetrical maxima, indicative of monoclinic symmetry.

Figure 11 presents plots of optic c-axis orientations from samples 1 to 18. These samples exhibit concentrations of c-axes with highly intense point maxima positioned anticlockwise from the normal to the shear plane, indicative of LT simple shear fabrics.

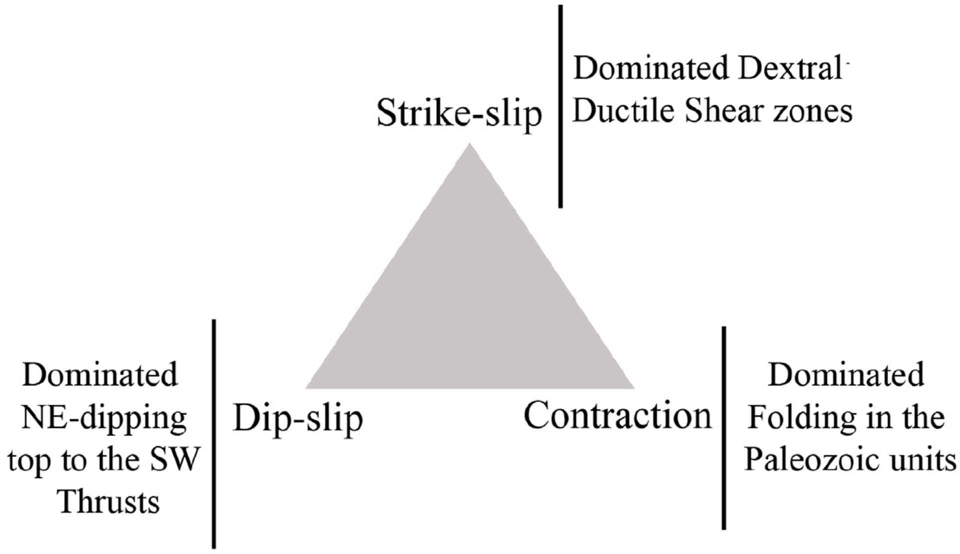

FIGURE 9
Structural relationships in the Bazar area, illustrating direct correlations with contractional, dip-slip, and strike-slip components as outlined by the strain triangle in the inclined transpression model (Jones, 2004). A clearer structural strain model, similar to that proposed by Xiao et al. (2023), is used to better depict the control of deformation partitioning in the region. This model provides a more comprehensive understanding of the structural evolution and its implications for deformation processes.

4.3 Paleostress orientations from calcite twins

Data were organized into distinct files for c-axes, e-twin lamellae, compression directions, and tension directions, formatted for immediate application in stereographic projection software. In instances where a calcite grain features two or three e-twin lamellae, the corresponding c-axis data for that grain is recorded multiple times in the dataset (Shelley, 1989; Shelley, 1993). Figure 11 illustrates the orientations of c-axes alongside the derived compression and tension directions. These orientations of the principal stress axes were determined by analyzing twin plane and c-axis measurements to deduce compression and tension directions for each analyzed grain. The aggregated data from all measured grains in the sample set were then contoured on an equal-area stereographic projection to display the results (Turner, 1953; Weiss, 1954; Pfiffner and Burkhard, 1987).

Figure 10 illustrates a monoclinic stress pattern derived from c-axes and twin planes data, where σ3 aligns with the tension axis maximum, and σ1 is close to the compression axis maximum. The compression axes (σ1) exhibit a NE–SW trend with shallow plunges ranging from 7°–19°, while the tension axes (σ3) display a NW–SE trend with moderate plunges of 12°–54°. Both stress axes, σ1 and σ3, are nearly horizontal, whereas the σ2 axis is predominantly vertical. These mean principal stress axes are mapped on a structural diagram, revealing a geometric alignment between compressional stress axes and thrusts, suggesting dextral movement in shear zones (Figures 5E–H).

The compressional stress indicated by calcite twinning in the Routshon complex is likely linked to the subduction of the Neotethys beneath the southern Sanandaj-Sirjan zone in central Iran during the Middle Triassic. Our findings suggest that a dextral inclined transpression regime was dominant in the metamorphic complexes within the hinterland of the Zagros orogen from the Middle Triassic to the Jurassic, associated with the oblique subduction of the Neotethys beneath central Iran. Notably, the Triassic-Early Jurassic σ1 trends observed in the Bazar area (this study) and the Faryab area (Shafieibafti, 2007) in the hinterland of the Zagros orogen align closely with the σ1 trend in the Fars province (Lacombe, 2007) of the Zagros Simply Folded Belt, located in the foreland of the Zagros orogen (resulting from the Mio-Pliocene Arabia–Eurasia collision). These consistent NE-SW orientations correlate with the current compressional trend in eastern and central Iran (Ebrahimi et al., 2021; Rashidi et al., 2021; 2023; Ezati et al., 2022; Rashidi and Derakhshani, 2022; Abbaspour et al., 2023), as shown in Figures 12A–E. Despite the significant time gap and the complex geodynamic context, this similarity in stress orientations may suggest that the stress regime in the upper plate (Zagros Simply Folded Belt) has remained relatively consistent from the onset of subduction in the Middle Triassic to the Mio-Pliocene Arabia–Eurasia collision (Shafieibafti, 2007).

4.4 Strengths and limitations of the data

Our study leverages a detailed analysis of calcite twinning and c-axis fabrics to interpret the tectonic evolution and paleostress patterns within the Routshon complex of the Sanandaj-Sirjan zone. The following points highlight the strengths and limitations of our data:

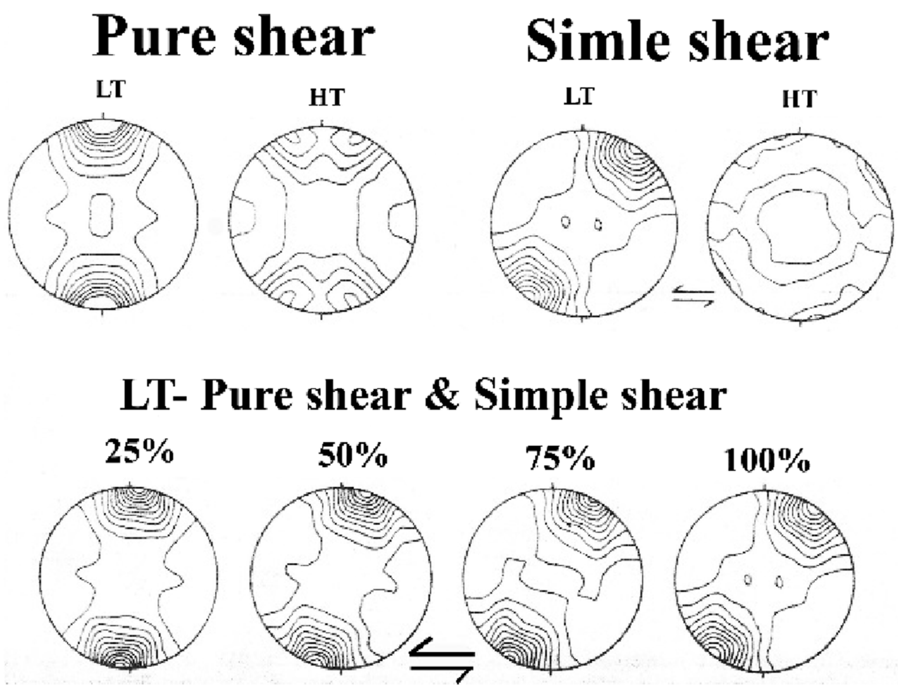

FIGURE 10
Computer simulations of c-axis fabrics in calcite based on experimental data, classifying these fabrics into low-temperature (LT) and high-temperature (HT) types. HT fabrics feature simple shear, evolving from rotated pure shear fabrics with added monoclinic distortion. LT fabrics, displayed in the lower part of the figure, consist of both pure shear and simple shear components, as oriented with respect to the external frame (Wenk et al., 1987).

4.4.1 Strengths

- Comprehensive Sampling and Analysis: The study is based on a dataset of 15 oriented samples of calcite mylonites from thrust-related shear zones. Each sample has been meticulously analyzed for c-axis orientations and twin lamellae using a U-stage, ensuring high accuracy and reliability of the data.
- Consistency with Experimental Findings: The observed low-temperature (LT) simple shear patterns in the c-axis fabrics align well with experimental studies, providing confidence in the interpretation of the shear sense and deformation mechanisms.
- Structural and Microstructural Correlations: Our interpretations are supported by detailed structural mapping and microstructural analysis, which reveal consistent geometries and kinematic indicators across multiple samples and outcrops.

4.4.2 Limitations

- Potential Rigid Body Behavior of Porphyroclasts: Under low-temperature conditions, porphyroclasts might behave as rigid bodies, potentially complicating the interpretation of ductile deformation. This aspect necessitates caution in interpreting the shear sense purely from calcite fabrics.
- Absence of EBSD Analysis: While Electron Backscatter Diffraction (EBSD) analysis could provide additional insights into the deformation mechanisms and validate our interpretations, it was not performed due to resource constraints. Future studies incorporating EBSD would help confirm our conclusions.
- Localized Data: The data and interpretations are derived from specific locations within the Routshon complex. While these findings provide valuable insights, they may not fully represent the broader regional deformation patterns and tectonic history.

5 Conclusion

The structural evolution observed in the study area is closely tied to slip partitioning, reflecting a comprehensive analysis within the domains of strike-slip, dip-slip, and contraction, as framed by the strain triangle model. The examination of optical c-axis orientations reveals pronounced point maxima, positioned anticlockwise from the normal to the shear plane, which indicates a low-temperature (LT) simple shear fabric. This LT fabric aligns with experimental findings, suggesting that twinning, is the predominant mechanism of deformation within the region. Further analysis identifies a dextral shear sense within mylonitic shear zones, characterized by a monoclinic stress pattern. This pattern is discernible through the orientation of c-axes and twin planes data, where σ_3 aligns with the tension axes' maximum and σ_1 is proximal to the compression axes' maximum. Notably, the compression axes (σ_1) exhibit a NE–SW orientation with shallow plunges ranging between 7°–19°, while the tension axes (σ_3) present a NW–SE trend with moderate plunges of 12°–54°. The orientations of σ_1 and σ_3 are predominantly sub-horizontal, while the σ_2 axis being sub-vertical. The plotted orientations of the mean principal stress axes on a structural map

10.3389/feart.2024.1445918

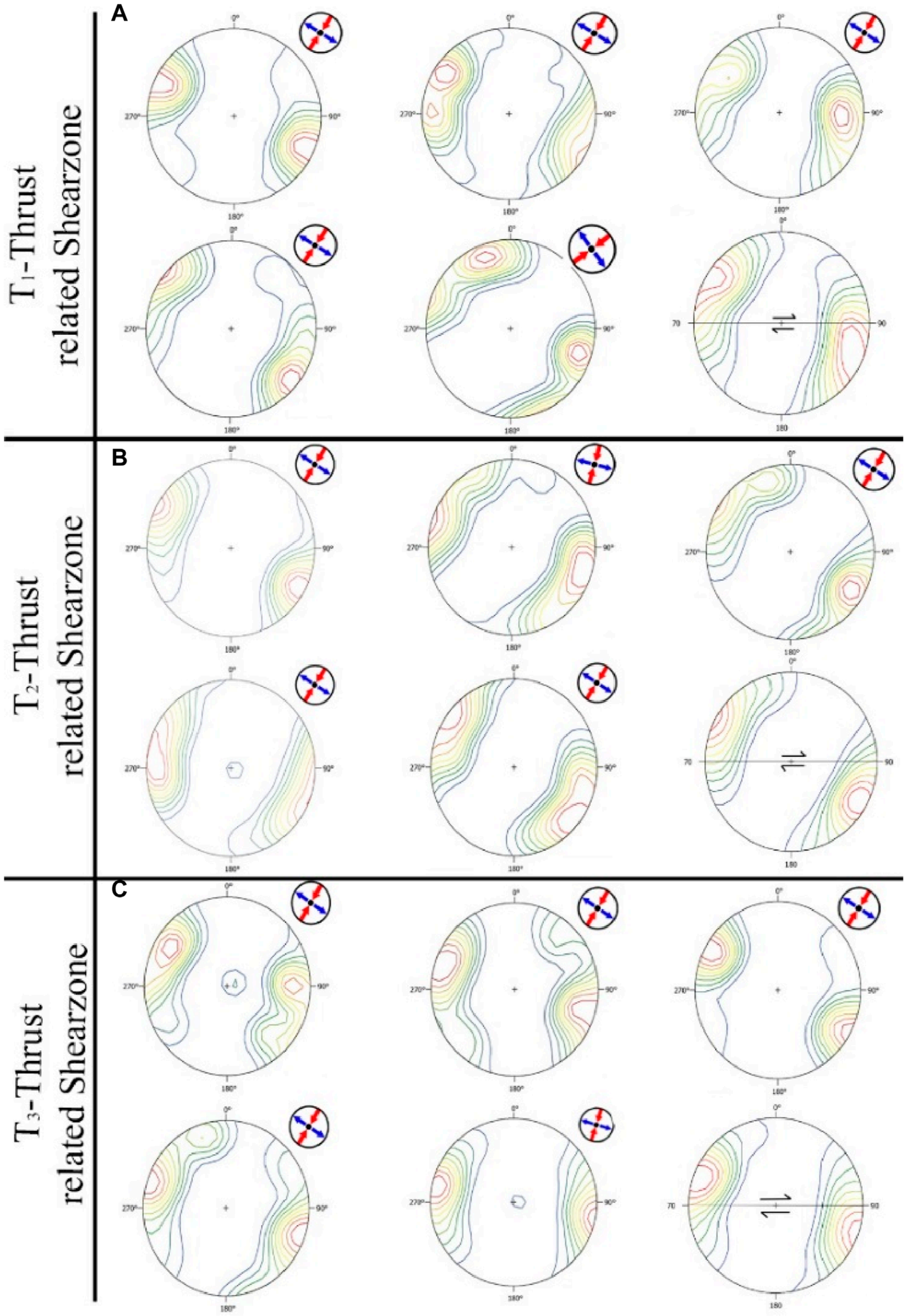

FIGURE 11
Presentation of calcite twinning data, showing orientations of c-axes, compression, and tension axes. Panels **(A–C)** illustrate c-axis fabrics displaying a low-temperature (LT) simple shear pattern, indicative of dextral shear sense in mylonitic shear zones. The data are plotted on lower hemisphere, equal-area stereographic projections with contour levels at 1%.

reveal a geometric relationship between compressional stress axes and thrusts, indicating a dextral movement across shear zones. Conclusively, the findings of this research confirm the prevalence of a dextral inclined transpression regime during the Middle Triassic-Jurassic period within the metamorphic complexes of the Zagros orogen hinterland.

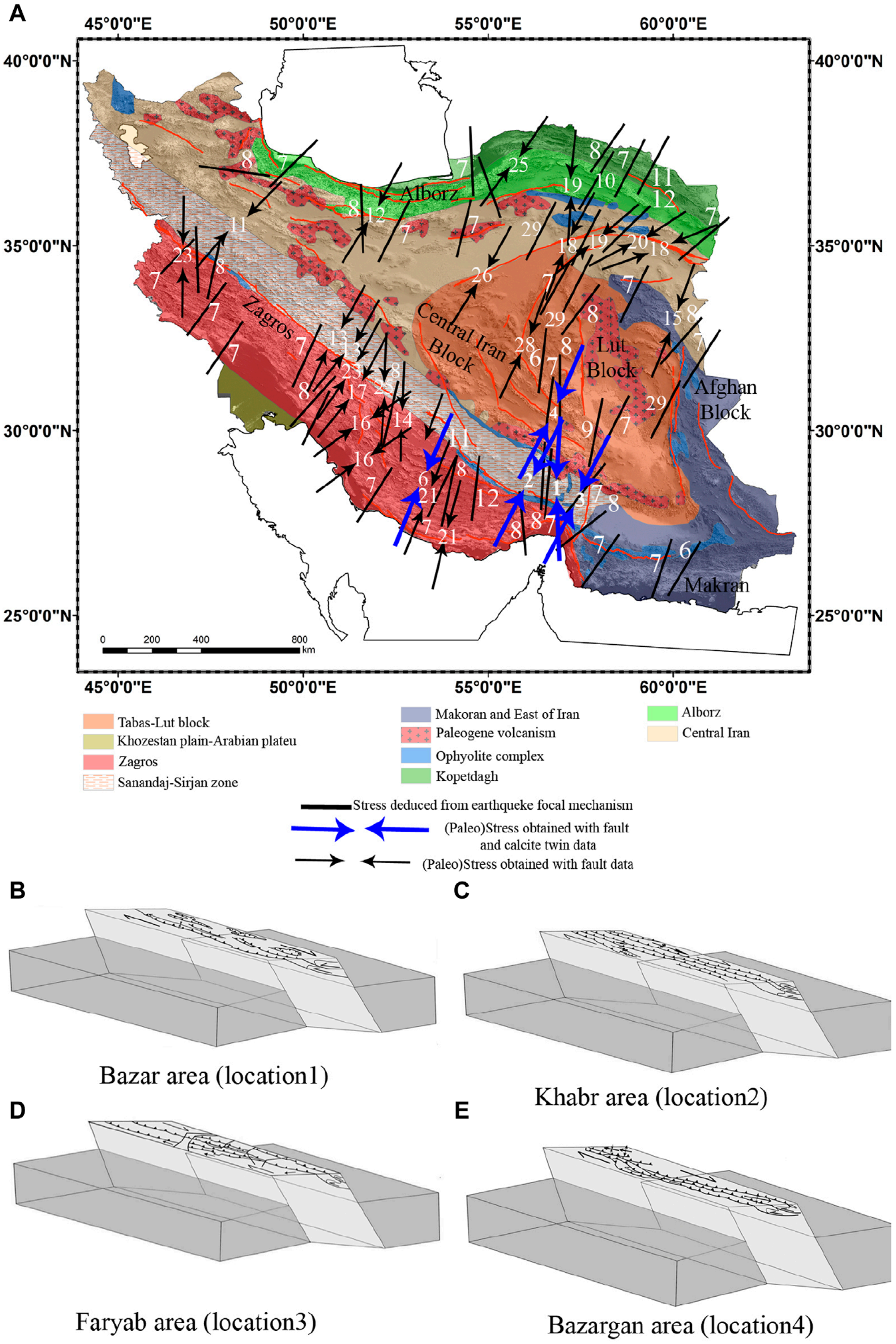

FIGURE 12
(A) Topographic map of Iran using SRTM 30 data, showing the orientation of compressive stress (azimuth of σ1). Different arrow styles represent various methodologies used to determine stress orientations. Key to methodologies: 1: this study; 2: (Shafieibafti and Mohajjel, 2015); 3: (Shafieibafti et al., 2011); 4: (Ebrahimi et al., 2021); 5: (Lacombe, 2007); 6: (Jentzer et al., 2017); 7: (Zarifi et al., 2014); 8: (Karagianni et al., 2015); 9: (Fattahpour and Moosavi, 2010); 10: (Zamani et al., 2008); 11: (Shabanian et al., 2010); 12: (Zanchi et al., 2006); 13: (Malekzade et al., 2016); 14: (Navabpour et al., 2008); 15: (Navabpour et al., 2007); 16: (Mobasher and Babaie, 2008); 17: (Authemayou et al., 2005); 18: (Javadi et al., 2013); 19: (Yazdi et al., 2012); 20: (Farbod et al., 2011); 21: (Lacombe et al., 2011); 22: (Authemayou et al., 2006); 23: (Navabpour and Barrier, 2012); 24: (Javidfakhr et al., 2011b; 2011a); 25: (Javadi et al., 2015); 26: (Kargaranbafghi et al., 2011); 27: (Lacombe et al., 2006); 28: (Dolati and Burg, 2013); 29: (Rashidi et al., 2022). **(B–E)** Schematic models illustrating inclined transpression within the Bazar, Khabr, and Faryab areas of the Sanandaj-Sirjan zone in the Zagros orogen hinterland, and the Bazargan area in the central Iran microcontinent, providing a comparative view of stress patterns and tectonic evolution across these regions.

Data availability statement

The original contributions presented in the study are included in the article/Supplementary Material, further inquiries can be directed to the corresponding authors.

Author contributions

HD: Formal Analysis, Investigation, Software, Writing–original draft. SS: Conceptualization, Data curation, Methodology, Project administration, Supervision, Validation, Writing–original draft, Writing–review and editing. SK: Data curation, Methodology, Project administration, Supervision, Writing–review and editing. JO: Formal Analysis, Methodology, Supervision, Writing–review and editing. AR: Software, Validation, Visualization, Writing–review and editing. MN: Conceptualization, Validation, Visualization, Writing–review and editing. RD: Conceptualization, Funding acquisition, Resources, Supervision, Writing–review and editing.

Funding

The author(s) declare that no financial support was received for the research, authorship, and/or publication of this article.

Conflict of interest

The authors declare that the research was conducted in the absence of any commercial or financial relationships that could be construed as a potential conflict of interest.

Publisher's note

All claims expressed in this article are solely those of the authors and do not necessarily represent those of their affiliated organizations, or those of the publisher, the editors and the reviewers. Any product that may be evaluated in this article, or claim that may be made by its manufacturer, is not guaranteed or endorsed by the publisher.

References

Abbaspour, R., Mousavi, S. M., Rashidi, A., Khatib, M. M., and Shafieibafti, S. (2023). Tectonic paleostress field and its impact on the geodynamic evolution of Central Iran, case study: the Shotori Mountain. *J. Mt. Sci.* 20, 3018–3034. doi:10.1007/s11629-023-8017-6

Agard, P., Omrani, J., Jolivet, L., Whitechurch, H., Vrielynck, B., Spakman, W., et al. (2011). Zagros orogeny: a subduction-dominated process. *Geol. Mag.* 148, 692–725. doi:10.1017/S001675681100046X

Aghanabati, A. (2004). *Geology of Iran*. Tehran, Iran: Geological Survey of Iran Press.

Alavi, M. (1994). Tectonics of the Zagros orogenic belt of Iran: new data and interpretations. *Tectonophysics* 229, 211–238. doi:10.1016/0040-1951(94)90030-2

Alavi, M. (2004). Regional stratigraphy of the Zagros fold-thrust belt of Iran and its proforeland evolution. *Am. J. Sci.* 304, 1–20. doi:10.2475/ajs.304.1.1

Amirihanza, H., Shafieibafti, S., Derakhshani, R., and Khojastehfar, S. (2018). Controls on Cu mineralization in central part of the Kerman porphyry copper belt, SE Iran:constraints from structural and spatial pattern analysis. *J. Struct. Geol.* 116, 159–177. doi:10.1016/j.jsg.2018.08.010

Authemayou, C., Bellier, O., Chardon, D., Malekzade, Z., and Abassi, M. (2005). Role of the Kazerun fault system in active deformation of the Zagros fold-and-thrust belt (Iran). *Comptes Rendus. Géoscience* 337, 539–545. doi:10.1016/j.crte.2004.12.007

Authemayou, C., Chardon, D., Bellier, O., Malekzadeh, Z., Shabanian, E., and Abbassi, M. R. (2006). Late Cenozoic partitioning of oblique plate convergence in the Zagros fold-and-thrust belt (Iran). *Tectonics* 25, 1860. doi:10.1029/2005TC001860

Berberian, M. (1972). *Two important deformational and metamorphic phases in the belt northeast of the Zagros thrust line (Iran)*. Geological Survey of Iran. internal report (unpublished).

Berberian, M. (1973). Two important deformational and metamorphic phases in the belt northeast of the Zagros thrust line (Iran); a brief structural review of the Sanandaj-Sirjan belt. *Geol. Surv. Iran. Intern. Rep.* 21 (7), 829–843.

Berberian, M. (1976). An explanatory note on the first seismotectonic map of Iran, a seismotectonic review of the country. *Contribution to the seismotectonic of Iran (Part III). Geol. Surv. Iran.* 39, 7–141.

Berberian, M., and King, G. C. P. (1981). Towards a paleogeography and tectonic evolution of Iran. *Can. J. Earth Sci.* 18, 210–265. doi:10.1139/e81-019

Berberian, M., and Nogol, M. (1974). *Preliminary explanation text of the geology of Deh Sard and Khabr maps with some remarks on the metamorphic complexes and the tectonics of the area (two geological maps, 1/100000 from the Hajiabad quadrangle map)*. Tehran, Iran: Geological Survey of Iran. Geol Survey of Iran Int Rep, 1–60.

Burkhard, M. (1993). Calcite twins, their geometry, appearance and significance as stress-strain markers and indicators of tectonic regime: a review. *J. Struct. Geol.* 15, 351–368. doi:10.1016/0191-8141(93)90132-T

Derakhshani, R., and Eslami, S. S. (2011). A new viewpoint for seismotectonic zoning. *Am. J. Environ. Sci.* 7, 212–218. doi:10.3844/ajessp.2011.212.218

Dolati, A., and Burg, J. P. (2013). Preliminary fault analysis and paleostress evolution in the makran fold-and-thrust belt in Iran. *Front. Earth Sci.* 5, 261–277. doi:10.1007/978-3-642-30609-9_13

Ebrahimi, Y., Shafieibafti, S., Derakhshani, R., and Esmaeilian, S. (2021). Slip partitioning and inclined transpression in the Bazargan fold and thrust belt, Central Iran Microcontinent, Kerman area, SE Iran. *J. Struct. Geol.* 148, 104352. doi:10.1016/j.jsg.2021.104352

Evans, M. A., and Groshong, R. H. (1994). A computer program for the calcite strain-gauge technique. *J. Struct. Geol.* 16, 277–281. doi:10.1016/0191-8141(94)90110-4

Ezati, M., Rashidi, A., Gholami, E., Mousavi, S. M., Nemati, M., Shafieibafti, S., et al. (2022). Paleostress analysis in the Northern Birjand, East of Iran: insights from inversion of fault-slip data. *Minerals* 12, 1606. doi:10.3390/min12121606

Falcon, N. L. (1961). Major earth-flexuring in the Zagros mountains of south-west Iran. *Q. J. Geol. Soc.* 117, 367–376. doi:10.1144/gsjgs.117.1.0367

Farbod, Y., Bellier, O., Shabanian, E., and Abbassi, M. R. (2011). Geomorphic and structural variations along the doruneh fault system (central Iran). *Tectonics* 30, 2889. doi:10.1029/2011TC002889

Fattahpour, V., and Moosavi, M. (2010). Stress inversion from the focal mechanism solution of Bam earthquake aftershocks (Iran, 2003). *J. Geophys. Eng.* 7, 290–301. doi:10.1088/1742-2132/7/3/008

Ghanbarian, M. A., and Derakhshani, R. (2022a). Systematic variations in the deformation intensity in the Zagros Hinterland Fold-and-Thrust Belt, Iran. *Z. Dtsch. Ges. fur Geowiss.* 173, 193–210. doi:10.1127/zdgg/2021/0276

Ghanbarian, M. A., and Derakhshani, R. (2022b). The folds and faults kinematic association in Zagros. *Sci. Rep.* 12, 8350. doi:10.1038/s41598-022-12337-8

Ghanbarian, M. A., Yassaghi, A., and Derakhshani, R. (2021). Detecting a sinistral transpressional deformation belt in the Zagros. *Geosci. (Basel)* 11, 226. doi:10.3390/geosciences11060226

Ghasemi, A., and Talbot, C. J. (2006). A new tectonic scenario for the Sanandaj–Sirjan Zone (Iran). *J. Asian Earth Sci.* 26, 683–693. doi:10.1016/j.jseaes.2005.01.003

Ghazi, J. M., and Moazzen, M. (2015). Geodynamic evolution of the Sanandaj-Sirjan zone, Zagros orogen, Iran. *Turkish J. Earth Sci.* 24, 513–528. doi:10.3906/yer-1404-12

GSI (1997a). *Geological map of gol-e-gohar*. Iran: Tehran.

GSI (1997b). *Geological map of Khabr*. Iran: Tehran.

GSI (2007). *Geological map of bazar*. Iran: Tehran.

Handin, J. W., and Griggs, D. (1951). Deformation of Yule marble: Part II—predicted fabric changes. *Geol. Soc. Am. Bull.* 62, 863–886. doi:10.1130/0016-7606(1951)62[863:doympi]2.0.co;2

Hatcher, R. D. (1995). *Structural geology: principles, concepts, and problems*. United States: Prentice Hall.

Hatcher, R. D., and Hooper, R. J. (1992). "Evolution of crystalline thrust sheets in the internal parts of mountain chains," in *Thrust tectonics*. Egham, Surrey, England: University of London. doi:10.1007/978-94-011-3066-0_20

Hushmandzadeh, A., Sabzehi, M., and Breberian, M. (1972). *A brief note on Early Kimmerian orogeny and high grade metamorphism in the Sanandaj-sirjan Belt (Sirjan-Esfandagheh)*. Tehran, Iran: Geological Survey of Iran. Internal Report, 30.

Jamison, W. R., and Spang, J. H. (1976). Use of calcite twin lamellae to infer differential stress. *Geol. Soc. Am. Bull.* 87, 868. doi:10.1130/0016-7606(1976)87<868:UOCTLT>2.0.CO;2

Javadi, H. R., Esterabi Ashtiani, M., Guest, B., Yassaghi, A., Ghassemi, M. R., Shahpasandzadeh, M., et al. (2015). Tectonic reversal of the western doruneh fault system: implications for Central Asian tectonics. *Tectonics* 34, 2034–2051. doi:10.1002/2015TC003931

Javadi, H. R., Ghassemi, M. R., Shahpasandzadeh, M., Guest, B., Ashtiani, M. E., Yassaghi, A. L. I., et al. (2013). History of faulting on the doruneh fault system: implications for the kinematic changes of the central Iranian microplate. *Geol. Mag.* 150, 651–672. doi:10.1017/S0016756812000751

Javidfakhr, B., Bellier, O., Shabanian, E., Ahmadian, S., and Saidi, A. (2011a). Plio-Quaternary tectonic regime changes in the transition zone between Alborz and Kopeh Dagh mountain ranges (NE Iran). *Tectonophysics* 506, 86–108. doi:10.1016/j.tecto.2011.04.013

Javidfakhr, B., Bellier, O., Shabanian, E., Siame, L., Léanni, L., Bourlès, D., et al. (2011b). Fault kinematics and active tectonics at the southeastern boundary of the eastern Alborz (Abr and Khij fault zones): geodynamic implications for NNE Iran. *J. Geodyn.* 52, 290–303. doi:10.1016/j.jog.2011.02.005

Jaya, A., and Nishikawa, O. (2013). Paleostress reconstruction from calcite twin and fault-slip data using the multiple inverse method in the East Walanae fault zone: implications for the Neogene contraction in South Sulawesi, Indonesia. *J. Struct. Geol.* 55, 34–49. doi:10.1016/j.jsg.2013.07.006

Jentzer, M., Fournier, M., Agard, P., Omrani, J., Khatib, M. M., and Whitechurch, H. (2017). Neogene to Present paleostress field in Eastern Iran (Sistan belt) and implications for regional geodynamics. *Tectonics* 36, 321–339. doi:10.1002/2016TC004275

Jones, S. J. (2004). Tectonic controls on drainage evolution and development of terminal alluvial fans, southern Pyrenees, Spain. *Terra Nova.* 16, 121–127. doi:10.1111/j.1365-3121.2004.00539.x

Kamali, Z., Nazari, H., Rashidi, A., Heyhat, M. R., Khatib, M. M., and Derakhshani, R. (2023). Seismotectonics, geomorphology and paleoseismology of the doroud fault, a source of seismic hazard in Zagros. *Appl. Sci.* 13, 3747. doi:10.3390/app13063747

Karagianni, I., Papazachos, C. B., Scordilis, E. M., and Karakaisis, G. F. (2015). Reviewing the active stress field in Central Asia by using a modified stress tensor approach. *J. Seismol.* 19, 541–565. doi:10.1007/s10950-015-9481-4

Kargaranbafghi, F., Neubauer, F., and Genser, J. (2011). Cenozoic kinematic evolution of southwestern Central Iran: strain partitioning and accommodation of Arabia-Eurasia convergence. *Tectonophysics* 502, 221–243. doi:10.1016/j.tecto.2010.02.004

Kermani, A. F., Derakhshani, R., and Shafieibafti, S. (2017). Data on morphotectonic indices of Dashtekhak district, Iran. *Data Brief.* 14, 782–788. doi:10.1016/j.dib.2017.08.052

Lacombe, O. (2001). Paleostress magnitudes associated with development of mountain belts: insights from tectonic analyses of calcite twins in the Taiwan foothills. *Tectonics* 20, 834–849. doi:10.1029/2001TC900019

Lacombe, O. (2007). Comparison of paleostress magnitudes from calcite twins with contemporary stress magnitudes and frictional sliding criteria in the continental crust: mechanical implications. *J. Struct. Geol.* 29, 86–99. doi:10.1016/j.jsg.2006.08.009

Lacombe, O., Bellahsen, N., and Mouthereau, F. (2011). Fracture patterns in the Zagros Simply Folded Belt (Fars, Iran): constraints on early collisional tectonic history and role of basement faults. *Geol. Mag.* 148, 940–963. doi:10.1017/S001675681100029X

Lacombe, O., and Laurent, P. (1992). Determination of principal stress magnitudes using calcite twins and rock mechanics data. *Tectonophysics* 202, 83–93. doi:10.1016/0040-1951(92)90456-G

Lacombe, O., and Laurent, P. (1996). Determination of deviatoric stress tensors based on inversion of calcite twin data from experimentally deformed monophase samples: preliminary results. *Tectonophysics* 255, 189–202. doi:10.1016/0040-1951(95)00136-0

Lacombe, O., Mouthereau, F., Kargar, S., and Meyer, B. (2006). Late Cenozoic and modern stress fields in the western Fars (Iran): implications for the tectonic and kinematic evolution of central Zagros. *Tectonics* 25, 1831. doi:10.1029/2005TC001831

Lafrance, B., White, J. C., and Williams, P. F. (1994). Natural calcite c-axis fabrics: an alternate interpretation. *Tectonophysics* 229, 1–18. doi:10.1016/0040-1951(94)90002-7

Majidi, B. (1972). Preliminary report of the hadjiabad quadrangle. Tehran: *Geol. Surv. Iran. Int. Rep*.

Majidi, B. (1974). Metamorphic problems of south Iran. *Memoirs Fac. Eng.*, 120–145.

Malekzade, Z., Bellier, O., Abbassi, M. R., Shabanian, E., and Authemayou, C. (2016). The effects of plate margin inhomogeneity on the deformation pattern within west-Central Zagros Fold-and-Thrust Belt. *Tectonophysics* 693, 304–326. doi:10.1016/j.tecto.2016.01.030

Mansouri, S. M., Keshavarz, S., Shahpasandzadeh, M., and Faghih, A. (2021). Strain and vorticity analyses using rotated porphyroclasts in the Tanbour metamorphic rocks: evidence of transpressional deformation along the Sanandaj-Sirjan metamorphic belt, SW Iran. *J. Struct. Geol.* 148, 104358. doi:10.1016/J.JSG.2021.104358

Mobasher, K., and Babaie, H. A. (2008). Kinematic significance of fold- and fault-related fracture systems in the Zagros mountains, southern Iran. *Tectonophysics* 451, 156–169. doi:10.1016/j.tecto.2007.11.060

Mohajjel, M., and Fergusson, C. L. (2000). Dextral transpression in Late Cretaceous continental collision, Sanandaj–Sirjan zone, western Iran. *J. Struct. Geol.* 22, 1125–1139. doi:10.1016/S0191-8141(00)00023-7

Mohajjel, M., Fergusson, C. L., and Sahandi, M. R. (2003). Cretaceous–Tertiary convergence and continental collision, Sanandaj–Sirjan zone, western Iran. *J. Asian Earth Sci.* 21, 397–412. doi:10.1016/S1367-9120(02)00035-4

MohammadiNia, A., Rashidi, A., Shafieibafti, S., Mousavi, S. M., Nemati, M., Kianimehr, H., et al. (2024). Unraveling the role of dextral faults in the formation of pull-apart basin structures and their implications on the genesis of ophiolites and pluto-volcanics. *Front. Earth Sci. (Lausanne)* 12, 1399447. doi:10.3389/feart.2024.1399447

Navabpour, P., Angelier, J., and Barrier, E. (2007). Cenozoic post-collisional brittle tectonic history and stress reorientation in the High Zagros Belt (Iran, Fars Province). *Tectonophysics* 432, 101–131. doi:10.1016/j.tecto.2006.12.007

Navabpour, P., Angelier, J., and Barrier, E. (2008). Stress state reconstruction of oblique collision and evolution of deformation partitioning in W-Zagros (Iran, Kermanshah). *Geophys J. Int.* 175, 755–782. doi:10.1111/j.1365-246X.2008.03916.x

Navabpour, P., and Barrier, E. (2012). Stress states in the Zagros fold-and-thrust belt from passive margin to collisional tectonic setting. *Tectonophysics* 581, 76–83. doi:10.1016/j.tecto.2012.01.011

Parsons, T., and Thompson, G. A. (1993). Does magmatism influence low-angle normal faulting? *Geology* 21, 247–250. doi:10.1130/0091-7613(1993)021<0247:dmilan>2.3.co;2

Pfiffner, O.-A., and Burkhard, M. (1987). Determination of paleostress axis orientations from fault, twin and earthquake data, *Annales tectonicae*, 1, 48–57.

Qiu, L., Kong, R., Yan, D. P., Mu, H. X., Sun, W., Sun, S., et al. (2022). Paleo–Pacific plate subduction on the eastern Asian margin: insights from the Jurassic foreland system of the overriding plate. *Bull. Geol. Soc. Am.* 134, 2305–2320. doi:10.1130/B36118.1

Qiu, L., Yan, D. P., Tang, S. L., Wang, Q., Yang, W. X., Tang, X., et al. (2016). Mesozoic geology of southwestern China: Indosinian foreland overthrusting and subsequent deformation. *J. Asian Earth Sci.* 122, 91–105. doi:10.1016/j.jseaes.2016.03.006

Rahbar, R., Shafieibafti, S., and Derakhshani, R. (2017). Investigation of the tectonic activity of Bazargan Mountain in Iran. *Sustain. Dev. Mt. Territ. 9* 9, 380–386. doi:10.21177/1998-4502-2017-9-4-380-386

Ramsay, J. G., and Huber, M. I. (1987). *The techniques of modern structural geology: folds and fractures*. 1st Edn. London, United Kingdom: Academic Press.

Rashidi, A., and Derakhshani, R. (2022). Strain and moment rates from GPS and seismological data in northern Iran: implications for an evaluation of stress trajectories and probabilistic fault rupture hazard. *Remote Sens. (Basel)* 14, 2219. doi:10.3390/rs14092219

Rashidi, A., Kianimehr, H., Shafieibafti, S., Mehrabi, A., and Derakhshani, R. (2021). Active faults in the west of the lut block (Central Iran). *Геофизические исследования* 22, 70–84. doi:10.21455/gr2021.3-5

Rashidi, A., Kianimehr, H., Yamini-Fard, F., Tatar, M., and Zafarani, H. (2022). Present stress map and deformation distribution in the NE lut block, eastern Iran: insights from seismic and geodetic strain and moment rates. *Pure Appl. Geophys* 179, 1887–1917. doi:10.1007/s00024-022-03015-x

Rashidi, A., Nemati, M., Shafieibafti, S., Pourbeyranvand, S., Derakhshani, R., and Braitenberg, C. (2023). Structure and kinematics of active faulting in the northern domain of Western and Central Alborz, Iran and interpretation in terms of tectonic evolution of the region. *J. Asian Earth Sci.* 255, 105760. doi:10.1016/J.JSEAES.2023.105760

Sabzehei, M., and Berberian, M. (1972). "Preliminary note on the structural and metamorphic history of the area between Dowlatabad and Esfandagheh, south-east Central Iran," in *Geol. Surv. Iran, internal report, first Iranian geological symposium*. Tehran: Iranian petroleum institute.

Sabzehei, M. S. (1974). *Les melange ophiolitiques de la region d'Esfandagheh*. France: These d'etate, Universite scientifique et medicale de Grenoble.

Sarkarinejad, K., and Azizi, A. (2008). Slip partitioning and inclined dextral transpression along the Zagros Thrust System, Iran. *J. Struct. Geol.* 30, 116–136. doi:10.1016/j.jsg.2007.10.001

Sarkarinejad, K., Faghih, A., and Grasemann, B. (2008). Transpressional deformations within the Sanandaj–Sirjan metamorphic belt (Zagros mountains, Iran). *J. Struct. Geol.* 30, 818–826. doi:10.1016/j.jsg.2008.03.003

Şengör, A. M. C., and Kidd, W. S. F. (1979). Post-collisional tectonics of the Turkish-Iranian plateau and a comparison with Tibet. *Tectonophysics* 55, 361–376. doi:10.1016/0040-1951(79)90184-7

Shabanian, E., Bellier, O., Abbassi, M. R., Siame, L., and Farbod, Y. (2010). Plio-quaternary stress states in NE Iran: Kopeh Dagh and Allah Dagh-Binalud mountain ranges. *Tectonophysics* 480, 280–304. doi:10.1016/j.tecto.2009.10.022

Shafieibafti, S. (2007). *Structural analysis of metamorphic rocks in the Faryab area (South of Esfandagheh)*. SE Iran Tehran, Iran: University of Shahid Beheshti, 129. Unpublished Ph. D. Thesis.

Shafieibafti, S., Alavi, S. A., and Mohajjel, M. (2011). Calcite twinning constraints on paleostress patterns and tectonic evolution of the Zagros hinterland: the Sargaz complex, Sanandaj–Sirjan zone, SE Iran. *Arabian J. Geosciences* 4, 1189–1205. doi:10.1007/s12517-010-0140-3

Shafieibafti, S., and Mohajjel, M. (2015). Structural evidence for slip partitioning and inclined dextral transpression along the SE Sanandaj–Sirjan zone, Iran. *Int. J. earth Sci.* 104, 587–601. doi:10.1007/s00531-014-1106-6

Shan, Y., Zheng, J., and Liang, X. (2019). Synthetic slip plane, the combination of a pair of twinned and untwinned e-planes in a single calcite crystal: application in dynamic analysis. *J. Struct. Geol.* 119, 81–92. doi:10.1016/j.jsg.2018.12.003

Sheikholeslami, M. R., Pique, A., Mobayen, P., Sabzehei, M., Bellon, H., and Emami, M. H. (2008). Tectono-metamorphic evolution of the Neyriz metamorphic complex, quri-kor-e-sefid area (Sanandaj-Sirjan zone, SW Iran). *J. Asian Earth Sci.* 31, 504–521. doi:10.1016/j.jseaes.2007.07.004

Shelley, D. (1989). CALCSTRESS: a program that calculates compression and tension directions from calcite u-stage data. *Comput. Geosci.* 15, 269–273. doi:10.1016/0098-3004(89)90040-X

Shelley, D. (1993). *Igneous and metamorphic rocks under the microscope: classification, textures, microstructures, and mineral preferred-orientations*. London, Chapman and Hall, United Kingdom.

Stocklin, J. (1968). Structural history and tectonics of Iran: a review. *Am. Assoc. Pet. Geol. Bull.* 52, 1229–1258. doi:10.1306/5D25C4A5-16C1-11D7-8645000102C1865D

Turner, F. J. (1953). Nature and dynamic interpretation of deformation lamellae in calcite of three marbles. *Am. J. Sci.* 251, 276–298. doi:10.2475/ajs.251.4.276

Turner, F. J., and Weiss, L. E. (1963). *Structural analysis of metamorphic tectonites*. New York: McGraw-Hill.

Twiss, R. J., and Moores, E. M. (1992). *Structural geology*. New York, United States: Macmillan.

Watters, W. A., and Sabzehei, M. (1970). Preliminary report, geology and topography of the metamorphic and igneous complex of the central part of the Neyriz Quadrangle. *Geol. Surv. Iran. Int. Rep.*, 253–269.

Weiss, L. E. (1954). *A study of tectonic style: structural investigation of a marble quartzite complex in southern California*, 30. United States: University of California Publications in Geological Science, 1–102.

Wenk, H. R., Takeshita, T., Bechler, E., Erskine, B. G., and Matthies, S. (1987). Pure shear and simple shear calcite textures. Comparison of experimental, theoretical and natural data. *J. Struct. Geol.* 9, 731–745. doi:10.1016/0191-8141(87)90156-8

Xiao, C. H., Chen, Z.L., Yao, X. F., Liu, X. C., and Liu, J. M. (2023). The control of deformation partitioning on gold mineralization in the Qingchengzi district, Liaodong Peninsula, northeastern China. *J. Asian Earth Sci.* 242, 105517. doi:10.1016/j.jseaes.2022.105517

Yamaji, A. (2015). How tightly does calcite e-twin constrain stress? *J. Struct. Geol.* 72, 83–95. doi:10.1016/j.jsg.2015.01.008

Yazdi, S. H. M., Pourkermani, M., Arian, M., and Karkheiran, A. (2012). Determination of stress orientation in sabzevar ophiolite zone in (khorasan razavi province, Iran). *Indian J. Sci. Technol.* 5, 1–6. doi:10.17485/ijst/2012/v5i10.6

Zamani, B., Angelier, J., and Zamani, A. (2008). State of stress induced by plate convergence and stress partitioning in northeastern Iran, as indicated by focal mechanisms of earthquakes. *J. Geodyn.* 45, 120–132. doi:10.1016/j.jog.2007.07.003

Zanchi, A., Berra, F., Mattei, M., Ghassemi, M. R., and Sabouri, J. (2006). Inversion tectonics in central Alborz, Iran. *J. Struct. Geol.* 28, 2023–2037. doi:10.1016/j.jsg.2006.06.020

Zarifi, Z., Nilfouroushan, F., and Raeesi, M. (2014). Crustal stress map of Iran: insight from seismic and geodetic computations. *Pure Appl. Geophys* 171, 1219–1236. doi:10.1007/s00024-013-0711-9

Zhang, Q., and Fossen, H. (2020). The dilemma of asymmetric porphyroclast systems and sense of shear. *J. Struct. Geol.* 130, 103893. doi:10.1016/j.jsg.2019.103893

Zheng, J., and Shan, Y. (2020). Inversion of polyphase calcite-twin data for deviatoric stress tensors: 2. Application to the Huangling Dome, northern South China. *J. Struct. Geol.* 138, 104089. doi:10.1016/j.jsg.2020.104089